N78-14578

MULTISPECTRAL SYSTEM ANALYSIS THROUGH MODELING AND SIMULATION*

W. A. Malila, J. M. Gleason, and R. C. Cicone**
Environmental Research Institute of Michigan
Ann Arbor, Michigan

ABSTRACT

The design and development of multispectral remote sensor systems and associated information extraction techniques should be optimized under the physical and economic constraints encountered and yet be effective over a wide range of scene and environmental conditions. Direct measurement of the full range of conditions to be encountered can be difficult, time consuming, and costly. Simulation of multispectral data by modeling scene, atmosphere, sensor, and data classifier characteristics is set forth as a viable alternative, particularly when coupled with limited sets of empirical measurements. A multispectral system modeling capability is described. Use of the model is illustrated for several applications -- interpretation of remotely sensed data from agricultural and forest scenes, evaluating atmospheric effects in Landsat data, examining system design and operational configuration, and development of information extraction techniques.

INTRODUCTION

Remotely sensed, multispectral scanner (MSS) data have been shown to be of value in a variety of applications related to earth resources surveys. The design and development of future scanner systems and related information extraction algorithms must be optimized under a variety of both physical and economic constraints to yield maximum amounts of information at a minimum cost for a particular application or a series of applications. In addition, optimal information extraction algorithms must be developed to utilize present scanner systems (e.g., Landsat) for applications of current interest. Such optimal development is extremely difficult, however, due to the wide range of parameters available to the scanner system designer, the wide range of scene characteristics of interest in a particular application, and the wide range of atmospheric conditions which may be encountered in an operational environment.

APPROACH

A viable approach to these difficult design and development problems is to simulate MSS data based on theoretical models of scene, atmospheric, scanner system, and data processor characteristics. Employing realistic measurements of the parameters required by these models, data can be generated at a relatively small expense over a wide range of conditions of interest. These data can then be analyzed for the purposes mentioned above. Simulated data can also be used to supplement empirical data obtained by an experimental or operational sensor system, to facilitate a greater understanding of those data.

*This work was supported by the National Aeronautics and Space Administration through their Earth Observations Division, Johnson Space Center, Houston, Texas, under Contract NAS9-14988.

**The authors are members of the Information Systems & Analysis Department, Infrared & Optics Division, ERIM, Ann Arbor, Michigan.

A Multispectral System Simulation Model has been developed at ERIM, based on previously developed capabilities for mathematically modeling the physical processes involved in the generation of remotely sensed signals. Outputs from the model have been employed for a variety of applications, some of which are illustrated later in the paper.

DESCRIPTION OF MODEL

The present basic components of the ERIM Multispectral System Simulation Model are:

(a) bidirectional reflectance model,

(b) atmospheric radiative transfer model,

(c) sensor system model, and

(d) data processor model.

An overall block diagram of the model is presented in Figure 1. The basic equation used to compute the spectral radiance L_λ observed by the scanner is:

$$L_\lambda = L_\lambda(S)\tau(\lambda) + L_\lambda(P)$$

where λ is wavelength,

$\tau(\lambda)$ is the spectral transmittance of the atmosphere along the path between surface and sensor,

$L_\lambda(P)$ is the spectral path radiance due to multiple scattering by the atmosphere along the path, and

$L_\lambda(S)$ is the spectral radiance emanating from the surface, i.e., the radiance before any atmospheric effects occur.

The surface radiance, in turn, depends on the direction and magnitude of irradiance at the surface, the scene bidirectional and diffuse reflectances, and the direction of observation. Specifically, the surface spectral radiance is:

$$L_\lambda(S, \theta_v, \psi_v, \theta_s, \psi_s) = \frac{1}{\pi} E_\lambda(\text{Direct}, \theta_s, \psi_s)\cdot\rho(\text{Bidirect}, \lambda, \theta_v, \psi_v, \theta_s, \psi_s) + E_\lambda(\text{Diffuse})\cdot\rho(\text{Diffuse},\lambda)$$

where $E_\lambda(\text{Direct})$ is the direct (solar) spectral irradiance,

$E_\lambda(\text{Diffuse})$ is the diffuse or hemispherical (sky) spectral irradiance,

$\rho(\text{Bidirect},\lambda)$ is the bidirectional spectral reflectance of the surface, relative to that of a horizontal, perfectly Lambertian surface,

$\rho(\text{Diffuse},\lambda)$ is the Lambertian spectral reflectance of the surface (i.e., response to a diffuse radiation source),

and (θ_v, ψ_v) and (θ_s, ψ_s) are the zenith and azimuth angles of view and sun, respectively.

Both the irradiance terms and the terms L_p and T depend on the properties of the atmosphere for the condition under consideration. In addition, $E_{Diffuse}$ and L_p depend on the albedo ρ_B of the background surrounding the surface element being viewed.

The bidirectional reflectance model used is that developed by Dr. G. H. Suits of ERIM [1,2]. This model computes the bidirectional reflectance of a vegetative canopy as a function of the spectral reflectance and transmittance characteristics of each of several canopy components and their sizes and average orientations within the canopy (i.e., horizontal and vertical projections of their cross-sectional areas). The basic model assumes that the canopy is infinite in extent and that its components are randomly oriented in layers. Computed values have agreed well with measured values in several instances [3-7]. Exceptions have been noted for row crops by two investigators [5,6]. Verhoef and Bunnik incorporated a crop row-effect parameter in a one-layer Suits' model and reported improved agreement between subsequently calculated and measured values [6]. In both References 6 and 7, certain discrepancies between modeled and measured reflectances have been attributed to specular leaf reflectances. Suits believes they could be a consequence of his use of only vertical and horizontal elements to represent leaf distributions and is developing a simple modification of his model to overcome this problem. Recently, Suits has added slope and aspect (i.e., azimuthal direction of slope) parameters to enable prediction of reflectances from canopies on sloping terrain (an example is presented later).

In the event that empirical measurement data are available, such as laboratory or field-measured reflectance spectra, these spectra can be utilized in simulation calculations in place of spectra computed theoretically with the reflectance model. Similarly, measured radiance spectra can be inserted at the appropriate place in the chain of calculations.

The atmospheric radiative transfer model is that developed by Dr. R. E. Turner of ERIM [8,9]. This model effectively has two parts, one which computes direct and diffuse solar irradiance spectra on a surface (at sea level or at any specified altitude), and the other which computes the spectral path radiance and spectral transmittance of the atmosphere along the path between the surface of interest and the sensor. These computed spectral quantities all depend on the state of the atmosphere and some depend also on sun position, view geometry, and/or background surface, as noted earlier. The diffuse irradiance term computed by the model includes all radiation scattered at least once by the atmosphere. Usually, this radiation has been assumed to be uniformly distributed throughout the hemisphere; however, it would be more accurate to take into account its actual spatial distribution which is concentrated in the aureole which surrounds the sun. The model assumes multiple scattering in a plane-parallel atmosphere. Absorption by aerosols can be included in the computation, although it usually has been omitted in calculations made. The most direct way to describe an atmospheric state for the model calculations is to input measured atmospheric optical thickness readings. Alternatively, one can utilize standardized atmospheric states which are labeled by their horizontal visual ranges.

The major component of the sensor system model is the set of functions that represent the relative spectral responses of the scanner's spectral channels. In the model, these can have arbitrary shapes as a function of wavelength. A radiance responsivity calibration option exists to convert effective inband radiances to sensor output units, and a sensor noise option is planned. For studies of satellite system operational considerations, an orbital model and sun position model permit one to predict system responses for a variety of orbit inclinations, equatorial crossing times, and scanning configurations.

Multispectral data classifier performance is simulated through a Monte Carlo technique based on statistics determined for the spectral classes of interest. Random samples are drawn from multiple scene-class populations and classified

into specified recognition classes using statistical decision rules. In addition to pure single-class pixels, multiclass mixture pixels which include field boundaries and/or spatial misregistration can be simulated [10].

APPLICATIONS OF MODEL

The multispectral system simulation capability described above has proven to be useful for a number of applications. Several representative uses are illustrated and described in this section, beginning with agricultural applications.

Knowledge of the effects of various factors on crop reflectance and their relative importance are both important in the design and development of processing techniques and procedures for crop inventory. Winter wheat is a crop that has a rather distinctive temporal development pattern relative to other crops and natural vegetation in the U.S. Great Plains. Wheat reflectance as a function of time was simulated using the model and field-measured wheat canopy component characteristics [11]. Seven growth stages, from emergence through harvest, were simulated (see Table I).

TABLE I. WHEAT GROWTH STAGES SIMULATED

Stage Number	Simulated Date	Wheat Growth Stage	Percent Growth Cover (Medium Density)
1	Mid November	Emergent	14
2	Mid April	Jointing	44
3	Mid May	Pre-heading	79
4	End May	Post-heading	82
5	Early June	Senescing	64
6	Late June	Ripe	60
7	Early July	Harvested	14

The sun position was chosen to match that at Landsat overpass time on each date at 38°N latitude. Atmospheric effects and Landsat inband radiances then were computed for several different atmospheric states. The resulting time tracks of wheat radiance in Landsat Bands 5 and 6 are presented in Figure 2 for one atmospheric state.

The family of plots in Figure 2 illustrates that wheat reflectance depends substantially on two canopy parameters -- density of vegetation, which differs from column to column in the array of plots, and soil brightness, which differs from row to row. The sparse, medium, and dense labels of canopy density apply on a relative basis at any given stage of development -- on an absolute basis, the dense canopy at emergence or post harvest had a lower percentage ground cover than did the sparse canopy at the time of full canopy development (i.e., at heading). Shadowing of exposed soil by the wheat leaves is another factor affecting the canopy reflectance. As one would expect, the soil brightness affected the total radiance most when ground cover percentage was lowest -- these and other simulated values serve to quantify the magnitude of the effect and indicate the variety of signature time tracks that are possible.

A related parametric study examined in more detail the characteristics of wheat reflectance during the "greening up" stages of wheat development [12]. Again, Landsat inband values were computed and analyzed. More levels of canopy

density were included through a parameter GLAI (Green Leaf Area Index) which is the total single-sided surface area of green leaves per unit area of ground. Figure 3 presents a family of curves for which GLAI varies from 0 (bare soil) to 26 (an extremely dense value to serve as a limiting case) with the mean soil brightness; typically mature wheat GLAIs are on the order of two to four, occasionally as high as six or eight. If GLAI were fixed, the percent ground cover and canopy reflectance could both vary, depending on the structure of the canopy. Canopy structure in the Suits model is implicit in the ratio of vertical to horizontal leaf area projections (V/H ratio) which also can be thought of as defining an average effective leaf orientation. The effect of varied V/H ratio is also displayed in Figure 3. (The actual V/H ratio of a wheat field will change throughout its development cycle.)

Families of curves for light, medium, and dark soil brightnesses are superimposed in Figure 4. For sparse canopies, the soil brightness is the predominant factor, while for dense canopies the V/H ratio predominates. Relatively small changes in reflectance occur when GLAI increases beyond a value of two. Alternative displays of the data in Figure 4 suggested that a polar coordinate description of the data would tend to decouple the effects of soil brightness and canopy density. Specifically, in Landsat reflectance space, an increase in soil brightness causes an increase in the radial component, while an increase in GLAI can be correlated with a counterclockwise rotation of a radial line through the origin. This rotation is both strikingly independent of soil brightness and not too sensitive to V/H changes. For Landsat signal space, a similar result is predicted but with a displacement of the origin of rotation due to path radiance effects. The polar angle for Figure 4 would be the angle whose tangent is the ratio of Band 7 to Band 5 reflectance, a quantity that has been found useful in Landsat analyses as a green vegetation indicator [e.g., 13-15].

The results presented here explain the reasons for the success of the 7/5 ratio and derivatives thereof and suggest that the polar angle, or a "green angle" measured from the radial line of bare soil, might provide a more linear measure of green vegetation density. Rather than utilizing just two of the four Landsat bands for defining the angular and radial components, linear combinations of all four such as those of the tasseled cap transformation [16] are recommended. The green angle is most closely related to the green component of the tasseled cap transformation.

The development of the tasseled cap transformation was based on calculations made using the Suits model, as well as analysis of empirical Landsat data. The majority of variance in Landsat data lies in the plane defined by the brightness and green axes. This transformation has proven to be a useful data processing technique and interpretation aid.

The above calculated reflectance values compared favorably with empirical values measured with a Landsat-band radiometer in wheat fields throughout a Kansas growing season, as shown in Figure 5.

Forests are frequently found in mountainous or hilly regions on sloping terrain. Slope and aspect do have pronounced effects on remotely sensed data. The slope and aspect parameters of the Suits model were used to predict the reflectance of a pine forest under various slope and aspect conditions. Figure 6 presents one set of results for Landsat Band 6 which indicated the extent to which the reflectance of a pine canopy is predicted to depart from that of a Lambertian (perfectly diffuse) surface.

Atmospheric effects are present in remotely sensed data acquired for all applications. An understanding of the magnitude and character of these effects is important to both the interpretation of data and the development of information extraction techniques and procedures. Figure 7 (reproduced from Reference 17) illustrates several facts about Landsat Band 4 data. First, path radiance

constitutes a large fraction of the signal from a target of medium reflectance (~8%). Second, the amount of atmospheric haze (indicated by horizontal visual range) affects the signal received. Finally, there are appreciable scan-angle-dependent effects even over the limited $\pm 6^{o}$ scan range of the Landsat MSS. Calculations of atmospheric effects can be tailored to the particular conditions and parameter values appropriate for any given application study.

The system model also has been used to examine the influence of scan geometry and system orbit parameters and sensor spectral characteristics on scanner responses [18]. In addition to atmospheric effects, the question of surface glint effects was addressed. Figure 8 presents a map of orbital coverage from 70^{o}N to 70^{o}S latitude along a ground track simulating the Thematic Mapper on an earlier proposed orbit with an 11:00 AM equator crossing. The cross-hatched zones indicate the surface slopes for which direct specular glint conditions could exist (e.g., from the sea surface) as a function of satellite latitude. By way of explanation, surface areas in the zone labeled $\geq 15^{o}$ would be susceptible to glint from any surface slope of 15^{o} or greater; the enclosed zones for $\geq 10^{o}$ and $\geq 5^{o}$ would be included as well in the potential glint region. The predicted glint potential for the currently planned 9:30 AM Thematic Mapper orbit is much less, with surface slopes of at least 20^{o} being required and the $\geq 20^{o}$ zone roughly matching the $\geq 10^{o}$ zone of Figure 8.

Figure 9 presents the nominal spectral bands of Thematic Mapper and Landsat MSS along with a reflectance spectrum of a green leaf to indicate the potential utility of the model in addressing problems of sensor spectral band selection. These problems require a consideration of atmospheric and viewing conditions and effects in addition to the spectral characteristics of scene surfaces.

Data processor simulation, based on signature statistics, is exemplified by previously reported predictions and analysis of the effects of spatial misregistration on classification performance [9].

SUMMARY

The ERIM Multispectral System Simulation Model has been described and several illustrative applications have been presented which address agricultural, forestry, general Landsat data interpretation and analysis, and system parameter selection problems. The capabilities described represent one implementation of a class of physical models which can play an important role in the continued development of remote sensing technology, especially when coupled with appropriate empirical measurements. The full potential of such modeling is yet to be realized.

ACKNOWLEDGEMENTS

The authors acknowledge the financial support of NASA and the technical support and consultation of other ERIM personnel, including R. F. Nalepka, R. J. Kauth, G. H. Suits, and R. E. Turner.

REFERENCES

1. Suits, G. H., 1972, "The Calculation of the Directional Reflectance of a Vegetative Canopy", Remote Sensing of Environment, Vol. 2, No. 2, pp. 117-125.

2. Suits, G. H., 1972, "The Cause of Azimuthal Variations in Directional Reflectance of Vegetative Canopies", Remote Sensing of Environment, Vol. 2, No. 3, pp. 175-182.

3. Suits, G. H., and G. R. Safir, 1972, "Verification of a Reflectance Model for Mature Corn with Applications to Corn Blight Detection", Remote Sensing of Environment, Vol. 2, No. 3, pp. 183-192.

4. Safir, G., G. Suits, and M. Wiese, 1972, "Application of a Directional Reflectance Model to Wheat Canopies under Stress", Proc. Intl. Conf. on Remote Sensing in Arid Lands, Tuscon, Ariz., Nov. 1972.

5. Malila, W. A., 1974, Information Extraction and Multiaspect Techniques in Remote Sensing, PhD Dissertation, The University of Michigan, Ann Arbor, Mich., Thesis Abstract 75-748, University Microfilms, Ann Arbor, Mich.

6. Verhoef, W., and N. J. Bunnik, 1976, The Spectral Directional Reflectance of Row Crops, Publication No. 35, NIWARS, Delft, Netherlands.

7. LeMaster, E. W., and J. E. Chance, 1977, "Further Tests of the Suits Reflectance Model", Eleventh Intl. Symp. on Remote Sensing of Environment, Environmental Research Institute of Michigan, Ann Arbor, Mich.

8. Turner, R. E., W. A. Malila, and R. F. Nalepka, 1971, "The Importance of Atmospheric Scattering in Remote Sensing...", Proc. of Seventh International Symposium on Remote Sensing of Environment, Pub. No. 10259-1-X, Willow Run Laboratories, The University of Michigan, Ann Arbor, Mich.

9. Turner, R. E., 1972, "Remote Sensing in Hazy Atmospheres", Proc. of ACSM/ASP Meeting, Washington, D.C., March 1972.

10. Cicone, R., W. Malila, and J. Gleason, 1976, "Effects of Misregistration on Multispectral Recognition", Proc. of Third Symposium on Machine Processing of Remotely Sensed Data, Purdue University, W. Lafayette, Ind.

11. Malila, W., R. Cicone, and J. Gleason, 1976, Wheat Signature Modeling and Analysis for Improved Training Statistics, ERIM 109600-66-F, Environmental Research Institute of Michigan, Ann Arbor, Mich.

12. Malila, W. and J. Gleason, "Task 4, Multicrop Remote Sensing Technique Development", Quarterly Progress Report for Period 15 Aug - 14 Nov 1976, submitted by R. Nalepka, Report 122700-11-L by Environmental Research Institute of Michigan, Ann Arbor, to NASA Johnson Space Center, Houston, Texas.

13. Colwell, J. E., 1973, Bidirectional Spectral Reflectance of Grass Canopies for Determination of Above Ground Standing Biomass, PhD Dissertation, The University of Michigan, Ann Arbor, Mich.

14. Wiegand, C., H. Gausman, J. Cuellar, and A. Gerbermann, 1973, "Vegetation Density as Deduced from ERTS-1 MSS Responses", Proc. of Third ERTS-1 Symposium, Greenbelt, Md, NASA SP-351.

15. Rouse, J., R. Haas, J. Schell, and D. Deering, 1973, "Monitoring Vegetation Systems in the Great Plains with ERTS", Proc. of Third ERTS-1 Symposium, Greenbelt, Md, NASA SP-351.

16. Kauth, R. J., and G. S. Thomas, 1976, "The Tasselled Cap -- A Graphic Description of the Spectral-Temporal Development of Agricultural Crops as Seen by Landsat", Proc. of 1976 Symposium on Machine Processing of Remotely Sensed Data, Purdue University, W. Lafayette, Ind.

17. Malila, W. A., and R. F. Nalepka, 1973, "Atmospheric Effects in ERTS-1 Data, and Advanced Information Extraction Techniques", Proc. of Symposium on Significant Results Obtained from ERTS-1, NASA SP-327, pp. 1097-1104.

18. Malila, W., J. Gleason, and R. Cicone, 1976, Final Report on Atmospheric Modeling Related to Thematic Mapper Scan Geometry, NASA CR-147792, NTIS No. N76-26675, ERIM 119300-5-F, Environmental Research Institute of Michigan, Ann Arbor, Mich.

FIGURE 1

ERIM MULTISPECTRAL SYSTEM SIMULATION MODEL

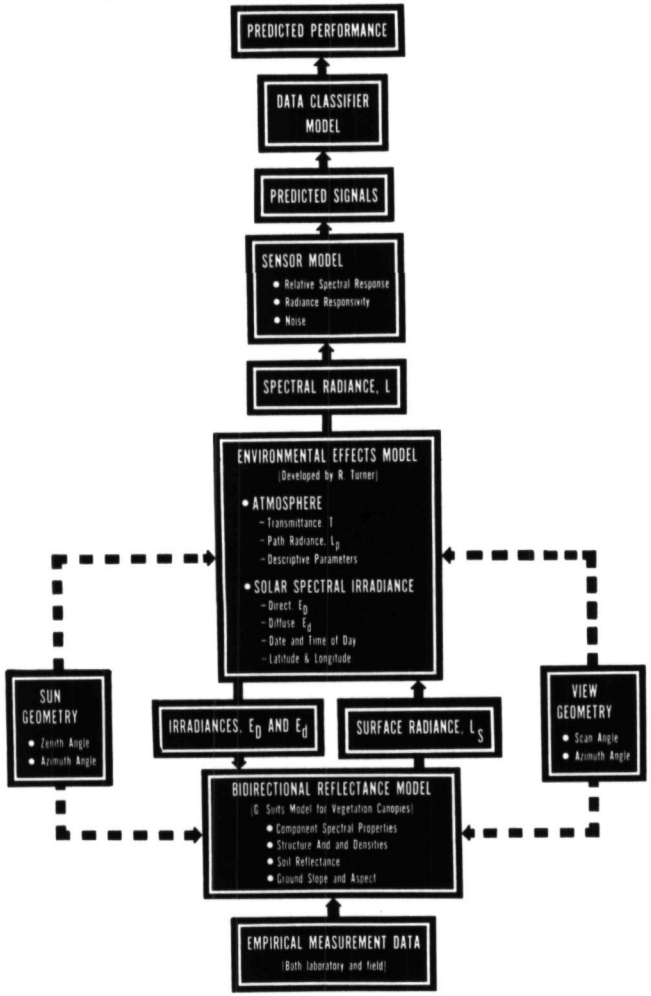

FIGURE 2

TEMPORAL TRACKS OF SIMULATED WHEAT CANOPY RADIANCE SIGNATURES IN LANDSAT BANDS (Key to growth stages is in Table I).

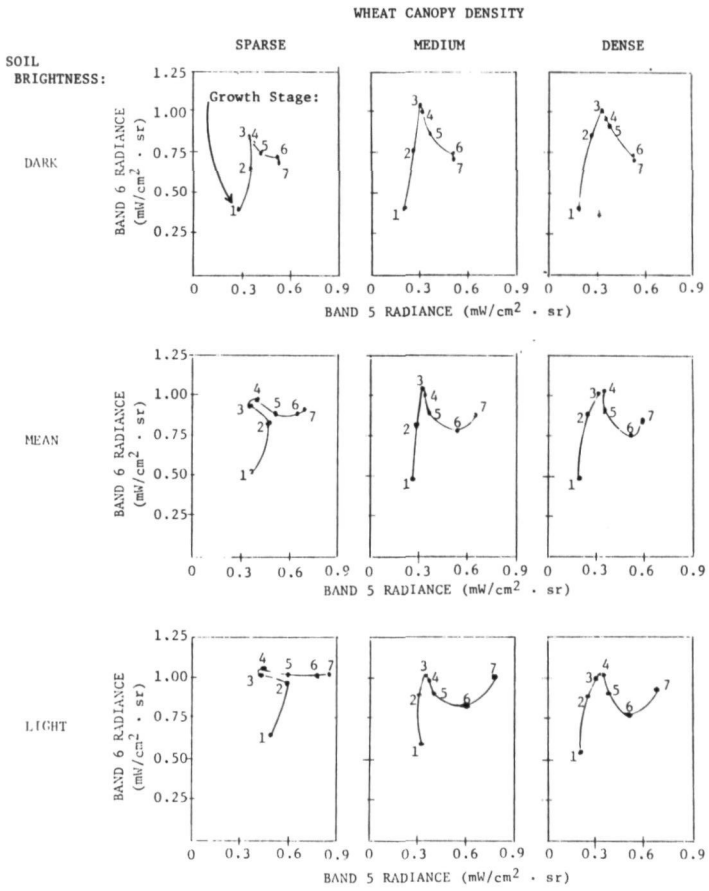

FIGURE 3

DEPENDENCE OF SIMULATED, LANDSAT INBAND, EMERGENT WHEAT CANOPY REFLECTANCE CHANGES (BAND 7 VERSUS 5) ON GREEN LEAF AREA INDEX (GLAI) FOR FIXED V/H RATIO AND MEAN SOIL BRIGHTNESS

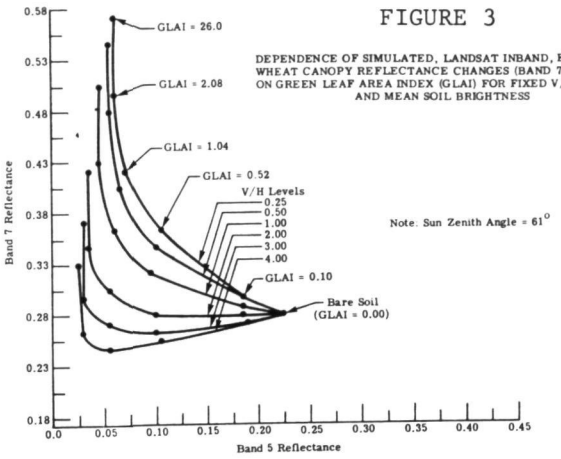

FIGURE 4

EFFECTS OF SOIL BRIGHTNESS ON SIMULATED, LANDSAT INBAND, EMERGENT WHEAT CANOPY REFLECTANCE CHANGES (BAND 7 VERSUS 5) AS GREEN LEAF AREA INDEX (GLAI) INCREASES, FOR FIXED V/H RATIOS

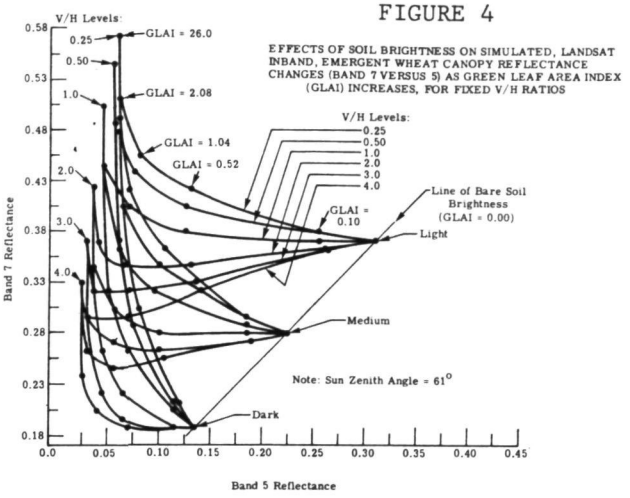

FIGURE 5

Comparison of Simulated and Empirical Reflectance Data

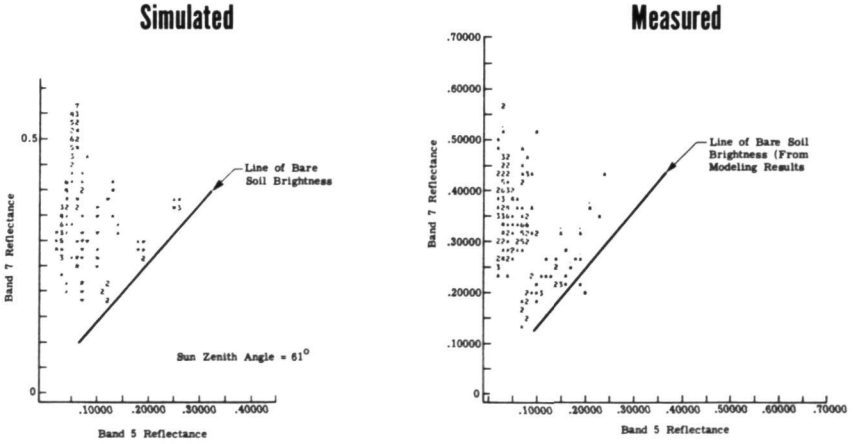

FIGURE 6

Interpretation of Data From Forested Areas

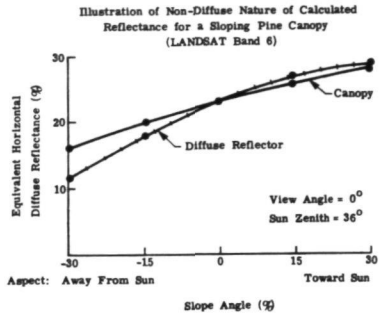

FIGURE 7

Prediction of Atmospheric Effects in LANDSAT Data

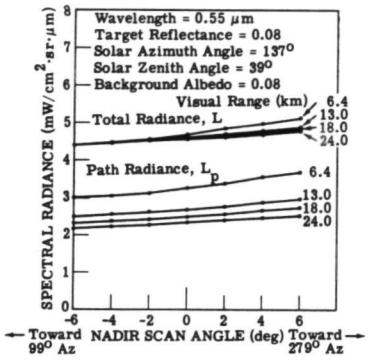

FIGURE 8

Sensor Orbit Selection

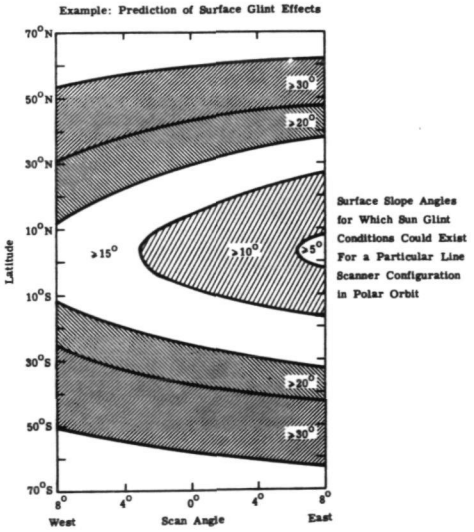

FIGURE 9

Sensor Spectral Band Selection